Materials Advances

ROYAL SOCIETY OF CHEMISTRY

PAPER

View Article Online
View Journal

Cite this: DOI: 10.1039/d5ma01299f

Cardanol-based benzoxazine and its potential with ammonium polyphosphate in flame-retardant coatings

Heng Jun Huei,[a] Wang Jiali,[a] Yen Zhihao,[a] Xiao Xingchi,[a] Ahmad Hedzir Fahmi bin Mohd Kamdi,[b] Rui A. Gonçalves[a] and Leonard Ng Wei Tat*[a]

Received 10th November 2025,
Accepted 31st December 2025

DOI: 10.1039/d5ma01299f

rsc.li/materials-advances

Polybenzoxazine is a versatile polymer that has high thermal stability, high char yield and inherent flame-retardant properties. Increasing attention is being paid to the synthesis of bio-based benzoxazines using renewable materials. This is attributed to the availability of phenols and primary amines in their precursors and the ability to rival their petroleum-based counterparts. A protocol for cardanol-based benzoxazine synthesis from cardanol and hexamethylenetetramine was optimised for scalability. The cardanol-based benzoxazine was then mixed with ammonium polyphosphate (APP) in different ratios to achieve flame retardancy. The results suggested that increasing the APP/benzoxazine ratio improved its flame retardancy and improved the density and homogeneity of the char layer.

1. Introduction

Wood, a material that is commonly used for furniture and construction, is usually treated to improve its properties such as chemical resistance, hydrophobicity and flame retardancy. As wood is very susceptible to burning, flame retardancy is vital for slowing down fire spread and increasing the escape time in the event of a fire. To achieve this, flame retardants are usually coated on the surface or impregnated into the wood.[1]

Polybenzoxazine, characterised by an oxazine ring connected to a benzene ring, is a type of thermosetting polymer with high potential for functionalisation.[2] Polybenzoxazine presents certain advantages, such as good thermal and mechanical properties[3] (high glass transition temperatures ranging from 170 to 340 °C, high tensile strength 100–125 MPa and storage modulus 3.8–4.5 GPa),[4] low water absorption, curing without requiring catalysts, and minimal shrinkage during curing.[5,6] Due to its high thermal stability and high char yield, it has been used for flame-retardant applications, such as in composites,[7] and intumescent coatings.[8] Beraldo *et al.* explored the use of benzoxazine as a binder for intumescent coatings due to its intrinsic flame retardancy attributed to the high aromatic content and the presence of a tertiary amine, achieving a surface treatment that decreased the substrate temperature by 300 °C.[8] Li *et al.* explored the use of benzoxazine as a synergist with ammonium polyphosphate in epoxy composites, achieving a limiting oxygen index of 31.3% with self-extinguishing capabilities and improved mechanical properties in 10% ammonium polyphosphate and 5% benzoxazine.[7] While research has been conducted on the use of benzoxazine as a binder and flame-retardant additive for flame-retardant coatings,[9] there have been few instances of benzoxazine acting as both a binder and an active ingredient in a coating system.

Recent advances have been made in the synthesis of bio-based benzoxazine, which uses more environmental friendly and renewable materials.[10–13] One such raw material explored is cardanol,[14–16] a component of cashew nut shell liquid, which is a byproduct of cashew nut processing. Oliveira *et al.* presented a microwave-assisted, formaldehyde-free benzoxazine synthesis using cardanol and hexamethylenetetramine (HMTA),[17] which is a safer, less toxic and more environmentally friendly method in comparison to conventional formaldehyde containing methods. While affording reactions at faster timescales, microwave reactions present some difficulties in upscaling, as they are prone to non-uniform heating and hotspots.[18–20]

An ingredient that is commonly used as a non-halogenated flame-retardant additive is ammonium polyphosphate (APP). At high temperatures, such as in the presence of a flame, APP degrades into phosphoric acid and phosphorus monoxide (PO) radicals.[21] These PO radicals combine with other highly reactive radicals produced during substrate degradation to suppress the flame.[22] In addition, phosphoric acid reacts with the hydroxyl groups in the decomposing polymer and catalyses dehydration to drive the formation of a protective heat-resistant carbonaceous

[a] School of Materials Science and Engineering, Nanyang Technological University, Singapore. E-mail: leonard.ngwt@ntu.edu.sg
[b] Evonik SEA Pte. Ltd., Singapore

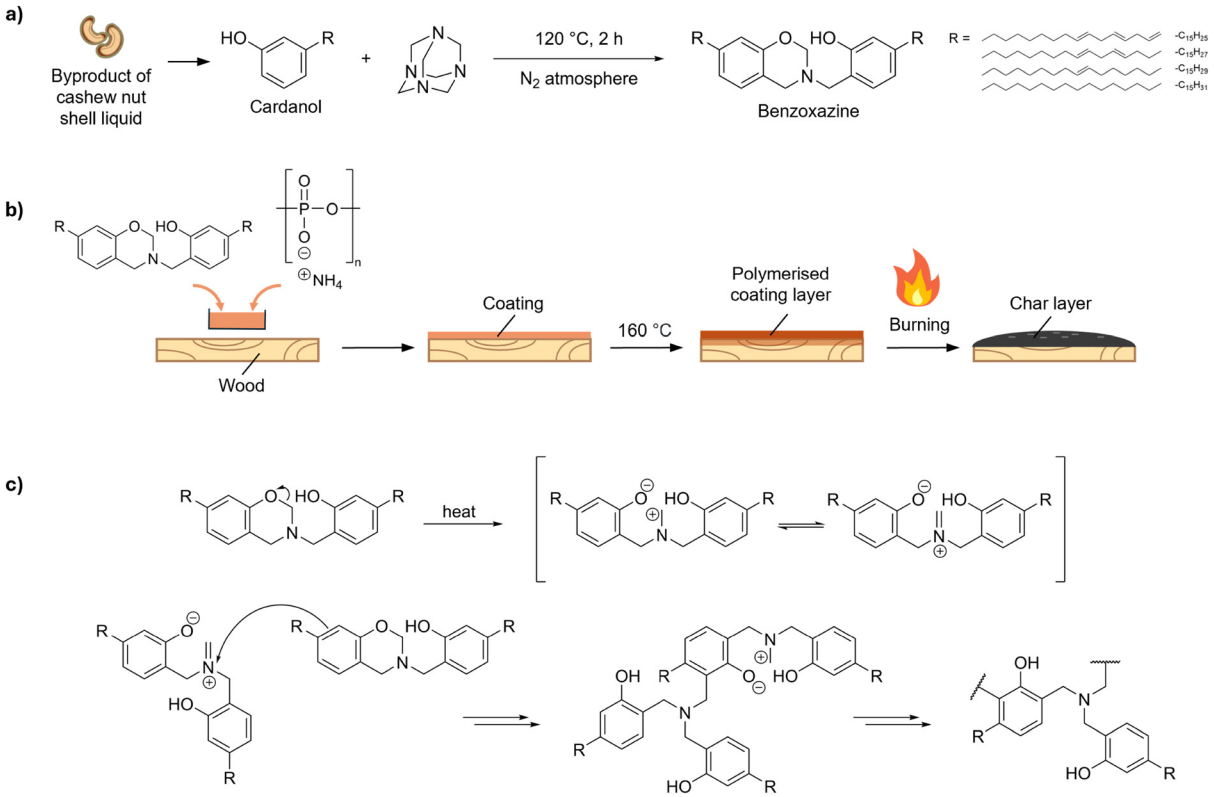

Fig. 1 (a) Schematic of benzoxazine synthesis. (b) Schematic of formulation, polymerisation and burning of coatings. (c) Ring-opening polymerisation of benzoxazine.

layer.[23] Mechanisms of the crosslinking of phosphate and hydroxyl groups in intumescent fire retardant systems during combustion have been proposed.[24,25] This strengthens the carbonaceous char layer produced, providing a heat-resistant barrier and protecting the substrate from the flame and heat. With hydroxyl groups present in benzoxazine, a synergistic reaction with the phosphate group in APP can occur.

Here, we present a protocol for cardanol-based benzoxazine synthesis using environmentally friendly materials at lower temperatures and reasonable timescales, without the need for further purification, and explore its potential with APP in flame-retardant wood coatings, as shown in Fig. 1a and b. Benzoxazine typically undergoes ring opening polymerisation to form polybenzoxazine,[26] as in Fig. 1c. Thermal ring opening polymerisation of benzoxazine results in the formation of a polybenzoxazine coating layer. Compared to the current baseline, this work presents a more scalable approach to benzoxazine synthesis with cardanol and HMTA and an investigation of benzoxazine as both the binder and active ingredient in flame-retardant coatings.

2. Experimental

To synthesise benzoxazine, the one pot formaldehyde-free synthesis protocol by Oliveira *et al.* from ref. 17 was modified by changing mode of heating, temperature conditions and duration. Cardanol (30 g, 0.10 mol) and hexamethylenetetramine (HMTA) (5.55 g, 0.04 mol) were added to a three-necked 150 mL round bottom flask under a nitrogen atmosphere and stirred at 120 °C for 2 h using a magnetic stirrer. After the reaction flask cooled, the product was diluted with ethyl acetate (150 mL) and the organic solution was washed with deionised water (4 × 150 mL) and brine (1 × 150 mL). The organic phase was collected, dried under anhydrous $MgSO_4$, concentrated *in vacuo*, and then left overnight in a vacuum oven at 40 °C, affording a dark orange oil with a viscosity of 5040 cP (at 25 °C and shear rate of 1 s^{-1}), named benzoxazine (31.9 g). Rheological characterisation is available in Fig. S1 of the SI.

For optimisation of the synthetic process, synthesis was performed in a range of temperatures, specifically at 160 °C, 140 °C, 130 °C, 120 °C, and 80 °C. The synthesis at 80 °C was deemed unsuccessful as thin layer chromatography (TLC) showed a large presence of starting reagent in the reaction mixture even after 3 h. The products from the remaining reactions were characterised using FTIR, DSC, and TGA and yielded similar results. However, at 160 °C, synthesis of benzoxazine yielded a highly viscous solid-like material after 2 h. From the differential scanning calorimetry (DSC) thermogram of benzoxazine in Fig. 2d, the gradient of the graphs turns positive at 130 °C, which suggested the possible onset of polymerisation. To prevent the occurrence of unfavourable polymerisation, we chose 120 °C as it is below this onset. Reaction completion at 2 h was determined using TLC. TLC characterisation is available in Fig. S2 of the SI.

We characterised the benzoxazine monomer using ^{1}H nuclear magnetic resonance spectroscopy (NMR), Fourier transform infrared spectroscopy (FTIR), DSC and thermogravimetric analysis (TGA). The benzoxazine monomer was then mixed with APP at different ratios using a speedmixer, applied onto wood panels using a 150-micron wire bar,[27,45] and polymerised in an oven (160 °C, 7h) The coatings were characterised using TGA, cone calorimeter tests and UL-94 vertical burning. The char residues were then observed under an optical microscope.

3. Results and discussion

3.1. Characterisation of the benzoxazine monomer

The chemical structure of benzoxazine was confirmed by ^{1}H NMR and FTIR (Fig. 2b and c). Comparing the NMR spectra of cardanol and benzoxazine in Fig. 2b, three new peaks at 4.87 ppm, 4.05 ppm and 4.01 ppm are observed, which are assigned to the resonances of the protons in O–CH_2–N, Benzyl–N–CH_2–Ar and Ar–CH_2–N–Oxazine and labelled a, b and c in Fig. 2b, respectively.[17] Comparing the integration of the aromatic protons, benzoxazine presents six aromatic protons, while cardanol presents four, consistent with the structure of benzoxazine. Further qualitative analysis and calculated conversion yield of benzoxazine are presented in Fig. S3 of the SI.

In Fig. 2c, a large reduction in the band intensity at 3344 cm^{-1} from the FTIR spectra of cardanol to benzoxazine is observed. This is likely due to the hydrogen bonding arising from the phenolic hydroxyl in cardanol. As two cardanol molecules in the reaction form a benzoxazine molecule, a hydroxyl group from a cardanol molecule establishes the ether bond, while the other cardanol hydroxyl likely forms an intramolecular hydrogen bond with the N in the tertiary amine, resulting in a weaker band at 3344 cm^{-1}. The bands at 1626 cm^{-1} and 1109 cm^{-1} are attributed to the trisubstituted benzene ring and the stretching of aromatic ether C–O–C, respectively, while the bands at 1191 cm^{-1} and 1163 cm^{-1} are attributed to the asymmetric stretching of C–N–C.[28] The band at 969 cm^{-1} is attributed to the oxazine skeletal vibrations and C–H out-of-plane bending.[29]

Comparing benzoxazines with identical structures,[13,16] in Table 2, the thermal characteristics are also similar. In the DSC thermogram presented in Fig. 2d, there are two exothermic events observed. The first peak at 247 °C is attributed to the ring opening polymerisation of benzoxazine, with an enthalpy of polymerization (ΔH_p) of approximately −54 J g^{-1} and a standard deviation of 6.2 from three runs. The second peak

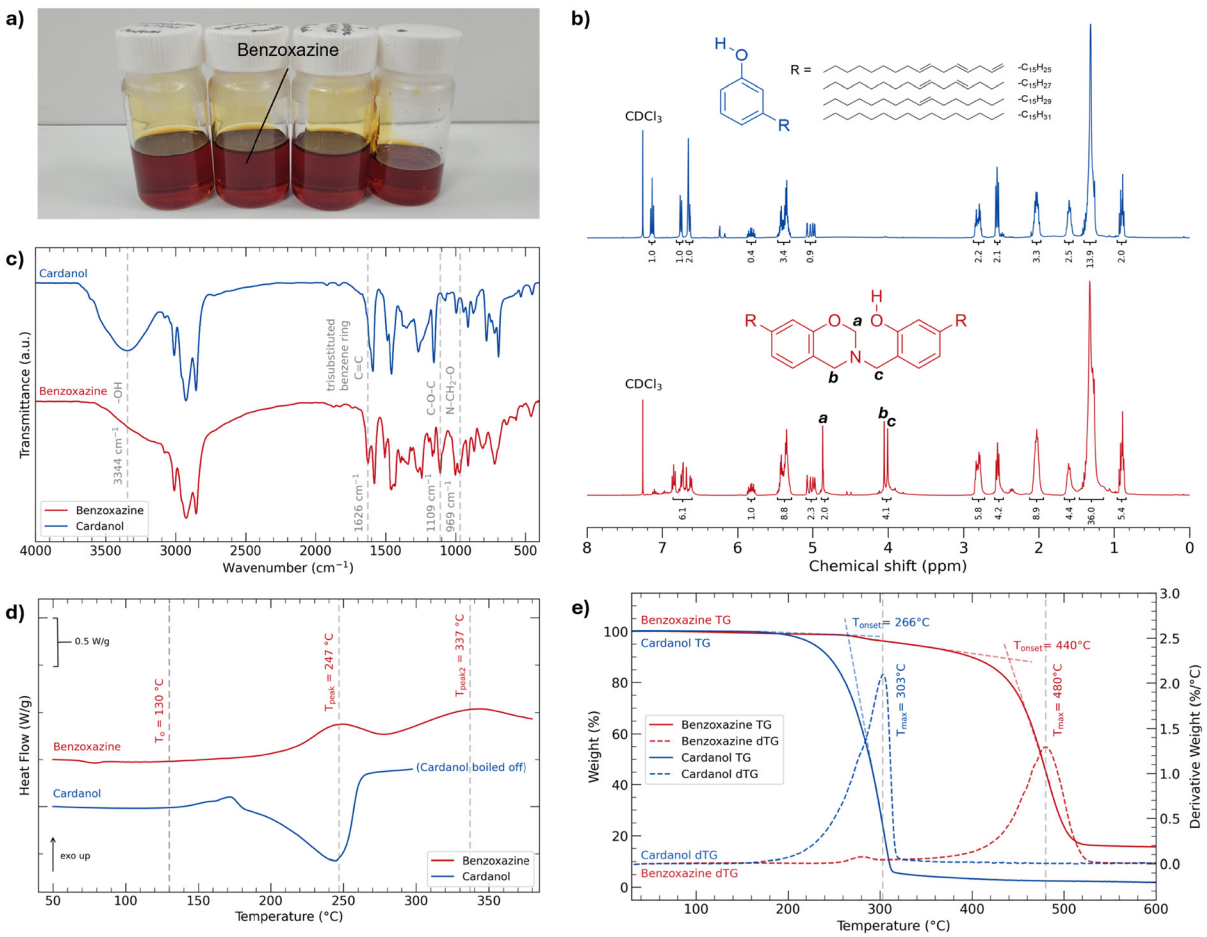

Fig. 2 Characterisation of the benzoxazine monomer (cardanol (blue) and benzoxazine (red)). (a) Optical image of benzoxazine. (b) ^{1}H NMR spectrum of cardanol (top) and benzoxazine (bottom). (c) FTIR spectra. (d) DSC at 10 °C min^{-1}. (e) TGA under a N_2 atmosphere at 20 °C min^{-1}.

Table 1 Formulation of coatings

Sample	APP (%)	Benzoxazine (%)
(0)	0	100
(1)	10	90
(2)	20	80
(3)	30	70
(4)	40	60
(5)	50	50
(6)	60	40

Table 2 Thermal properties of the benzoxazine monomer obtained from DSC analyses

	DSC			TGA	
Monomer	T_0 (°C)	T_{peak} (°C)	ΔH_p (J g^{-1})	T_{onset} (°C)	T_{max} (°C)
Benzoxazine	130	247	−54	440	480
CA-c[a]	215	247	−41	305	457
Bz[b]	—	243	−61	—	—

[a] As reported in ref. 17. [b] As reported in ref. 14.

at 337 °C is attributed to the oligomerisation of the unsaturated C═C in the side chain.[30] In the TGA thermogram presented in Fig. 2e, we observe the onset of degradation of benzoxazine at 440 °C and its peak degradation at 480 °C.

3.2. Characterisation of coatings

As plywood was the substrate used for the study, there were limitations on the temperature used for polymerisation, since plywood starts degrading at around 200 °C.[31] DSC and TGA thermograms of the wood substrate used for this study are also available in Fig. S4 and S5 of the SI. Benzoxazine was hence polymerised at 160 °C for a minimum of 7 h. DSC thermograms of polybenzoxazine are available in Fig. S6 of the SI. Comparing the FTIR spectrum of polybenzoxazine to that of benzoxazine in Fig. 3a, the successful polymerisation is confirmed from the disappearance of bands at 1109 cm^{-1} and 969 cm^{-1} which are attributed to the C–O–C stretching of the oxazine ring and the C–H out-of-plane bending of the benzene ring linked to the oxazine ring, respectively. Based on these results, benzoxazine was successfully polymerised at 160 °C for 7 h. FTIR spectra of the coatings are available in Fig. S7 of the SI.

The coatings were characterised using TGA for their thermal stability. The experiment was carried out under air flow to be more representative of the oxidising atmosphere present during combustion. The TGA thermograms and amount of residue are shown in Fig. 3b. TGA thermograms under N_2 flow are available in Fig. S8 of the SI. It can be seen that a higher percentage of APP generally correlates with a greater residue amount, with sample (0) giving the lowest residue at 4% and samples (1), (2), (3), (4), (5), and (6) leaving residues of 29%, 40%, 41%, 45%, 70%, and 60%, respectively. With a greater residue amount, the char layer that remains after the decomposition of other organic products is greater, having greater potential for fire retardancy.

The cone calorimeter test was used to investigate the combustion performance of the coatings and was set up as shown

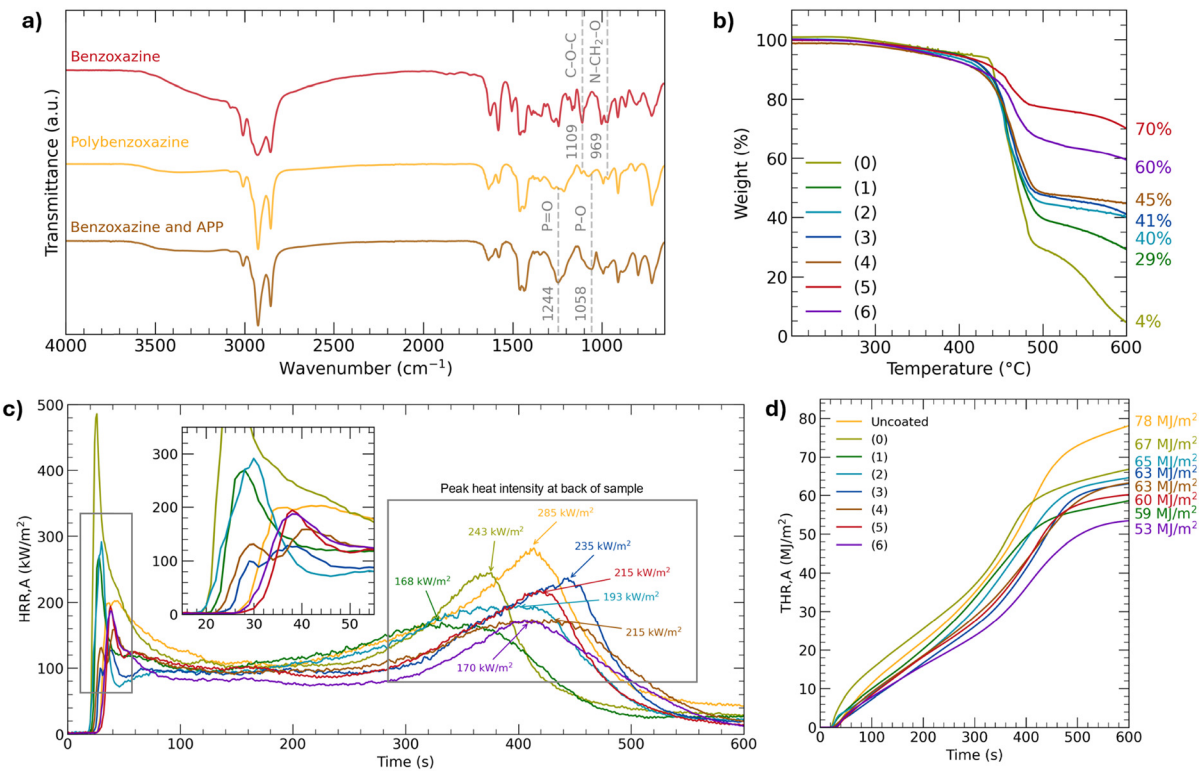

Fig. 3 Polymerisation and thermal characterisation of coatings. (a) FTIR spectra of benzoxazine (red), polybenzoxazine (yellow) and coating (brown). (b) TGA under air flow at 20 °C min^{-1}. (c) Heat release rate (HRR) of coatings. (d) Total heat release (THR) of coatings.

in Fig. S9 of the SI. The heat release rate (HRR) is calculated from the consumption of oxygen during the combustion of organic materials.[32] In the combustion of wood substrates, the first peak generally represents the full development of fire after the first ignition of the sample. After the first peak, a char layer that protects the substrate from the flames is formed, and the heat release rate remains relatively stable. The second peak corresponds to the point at which the heat reaches the back of the sample and the sample burns through.[33,34]

Fig. 3d shows that the heat release rate (HRR) generally decreases as the percentage of APP increases. In particular, at the second peak when the heat reaches the back of the sample, sample (6) performs best with an HRR of 170 kW m^{-2} (40% reduction) as compared to 285 kW m^{-2} of the uncoated sample. Sample (6) also has a stable section with an HRR of about 80 kW m^{-2}, which is lower as compared to that of the other samples ranging from 90 to 110 kW m^{-2}. The trend in total heat release (THR) in Fig. 3e is also consistent with the HRR, with sample (6) having the lowest THR at 53 MJ m^{-2} (32% reduction) and the uncoated sample having the highest THR at 78 MJ m^{-2}. The lower heat release capacity of sample (6) indicates the formation of an effective carbon char layer that inhibits heat release. The other samples (0), (1), (2), (3), (4), and (5) had the THR of 67 MJ m^{-2}, 59 MJ m^{-2}, 65 MJ m^{-2}, 63 MJ m^{-2}, 63 MJ m^{-2}, and 60 MJ m^{-2}, respectively, largely following the general trend. A lower HRR and THR correlate with lower probability of flame spread as less heat is supplied to its surroundings.[35] The THR of our samples are comparable to those of other polybenzoxazine materials, which are 100–130 MJ m^{-2} in ref. 36 and 48–72 MJ m^{-2} in ref. 37.

In the cone calorimeter test, samples were exposed to a cone heater and sparked using a spark igniter until sample ignition. The time to ignition is presented in Table 3. The results of the UL-94 vertical burning test (Table 3) remain consistent with those of the cone calorimeter test, where formulations with higher APP percentages display better flame retardancy. Afterflame times of the UL-94 tests can be found in Table S1 of the SI. It is noteworthy that the wood substrate is highly flammable and the coating must suppress and extinguish the flame, even if the coating does not ignite.

3.3. Characterisation of the char layer

The substrates were coated using a wire bar,[27,45] resulting in a wet film thickness of 150 μm, as depicted in Fig. 4a (top view) and Fig. 4b (side view). Fig. 4c displays the optical images of selected cone calorimeter test samples before and after burning. Top-down images of our samples after the cone calorimetry test are also available in Fig. S10 of the SI.

The surface morphology of the char layer is shown in the third row of Fig. 4c and d. The uncoated sample and Sample (0) exhibit similar morphologies, with the fibrous structure of the burnt wood clearly exposed. This observation is consistent with the TGA results for Sample (0), which show that polybenzoxazine underwent complete thermal degradation, leaving negligible residue.

Distinct morphologies are observed in the char layers of samples with varying APP content. Sample (1) shows a highly porous char layer, thus allowing greater heat transmission. In contrast, Sample (3) forms a denser char layer; however, compared to sample (6), it is uneven and contains numerous large pores or ruptures. These defects likely result from combustion gases breaching the surface, indicating an imperfect barrier. As the APP content increases in Sample (6), a more uniform and compact char layer was formed, with fewer cracks and large pores. This improved barrier likely accounts for its superior performance in the cone calorimeter test, characterised by the lower HRR and THR, as the stable carbonaceous char more effectively insulates the substrate from heat and flames.

Table 3 Time to ignition and UL-94 results of coatings

Samples	Cone calorimeter test	UL-94 vertical burning test	
	Average time to ignition (s)	Flaming dripping	UL-94 rating
Uncoated	19.0	No	No rating
(0)	12.3	No	No rating
(1)	14.3	No	No rating
(2)	13.3	No	V-1
(3)	19.3	No	V-1
(4)	18.7	No	V-1
(5)	22.0	No	V-0
(6)	21.0	No	V-0

3.4. Flame retardancy of coatings

The improved performance of the coatings in both the cone calorimeter and UL-94 vertical burning tests with increasing APP content could be attributed to two factors: the flame-retardant properties of APP and the potential crosslinking between phosphate groups and benzoxazine during combustion, leading to the formation of a stable carbonaceous char layer.

A phosphorus-to-hydroxyl ratio of 0.7 in composites has been reported to yield superior flame-retardant properties, including a higher limiting oxygen index and improved UL-94 rating, compared to other ratios.[24] However, in our system, the number of hydroxyl groups is insufficient to achieve this optimal ratio. Increasing the APP content could enhance the likelihood of crosslinking. This aligns with our findings, where higher APP loading resulted in increased residue formation and a more compact, denser char layer.

A higher APP content in the coatings generates greater amounts of incombustible gases and PO· radicals during thermal decomposition. These species dilute flammable gases and scavenge reactive radicals more effectively, thereby enhancing the quenching effect and overall flame-retardant performance.

4. Limitations and future work

This study focused on evaluating the flame retardancy of formulated coatings using a cone calorimeter and UL-94 vertical burning tests. Future research utilising high throughput experiments[38–41] on their behaviour during combustion should expand to include additional combustion-related properties such as smoke production and toxicity, limiting oxygen index,

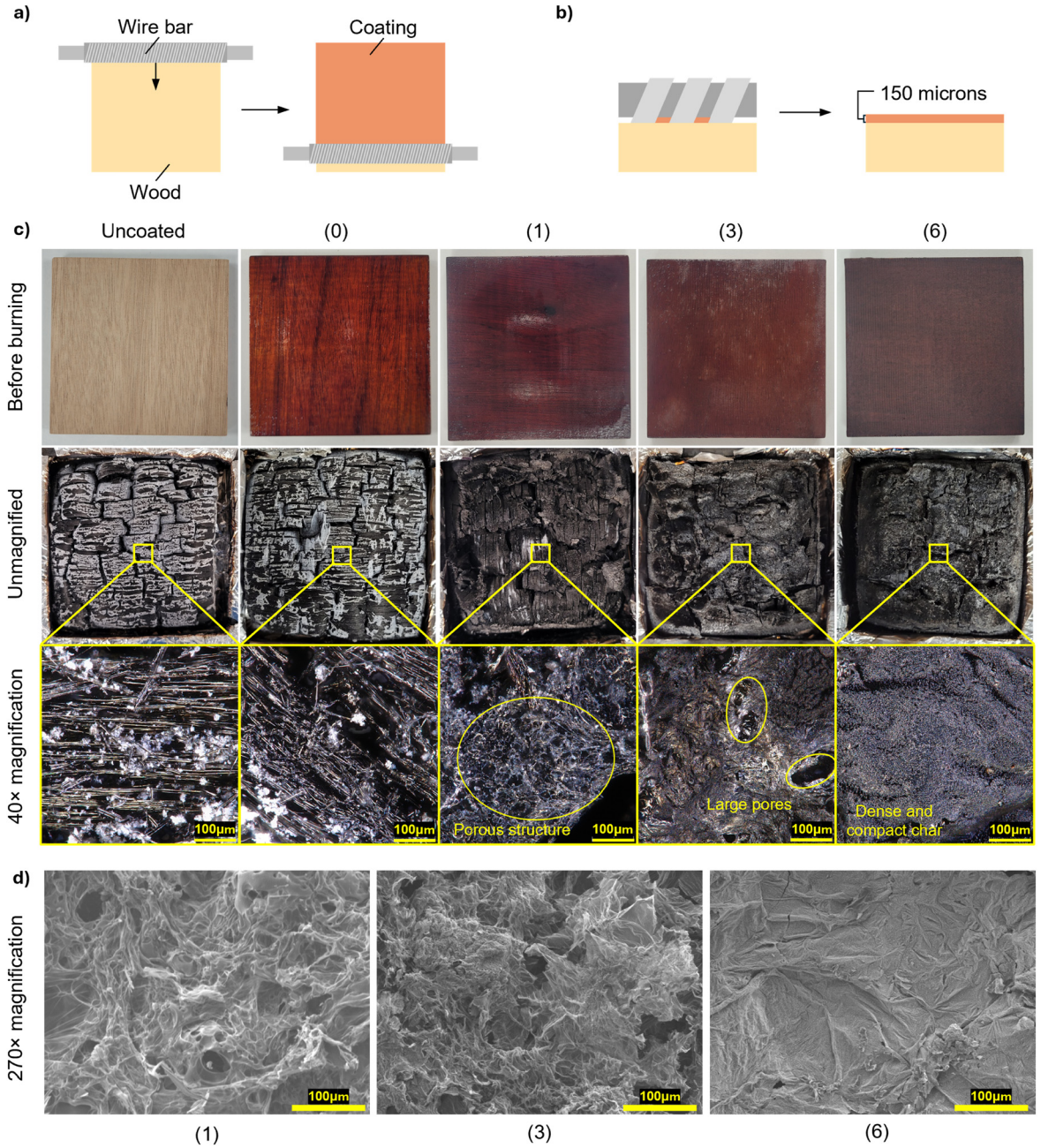

Fig. 4 Coating and char layer characterisation. (a) Schematic of wire bar drawdown coating (top view). (b) Schematic of wire bar drawdown (side view). (c) Optical images of samples before burning and optical microscopy images of samples after the cone calorimeter test. (d) SEM image of samples after the cone calorimeter test.

and horizontal burning. Moreover, other key performance properties such as hardness, scratch resistance, adhesion, hydrophobicity, and chemical resistance are crucial for coating applications and warrant further investigation. A systematic study on the properties of polybenzoxazine and the effects of flame-retardant additives on these properties would provide a more comprehensive understanding. The effect of coating thickness on char formation and thermal insulation could also be explored. The adhesion properties of the coating could be evaluated using methods such as scrape adhesion and pull-off tests to further infer on practical applications.[42]

A major limitation is that wood components such as cellulose and hemicellulose begin to decompose at temperatures below 200 °C, with irreversible reductions in mechanical strength reported at temperatures as low as 65 °C.[43] Consequently, the high temperatures required for the thermal ring-opening polymerisation of benzoxazine render it unsuitable for wood-based applications. High temperatures and long durations used for our curing process may have caused some degradation of the wood components. Some hydroxyl groups or carbonyl present in the wood components may have also cleaved off, reducing the flammability of the plywood itself.

Varying levels of mass loss and absorption of coating as a result may also contribute to the flame-retardance performance and evaluation of the coatings. Furthermore, given the small surface area of our wooden substrates and the varying porosity of wood, the final coating thickness may vary. Therefore, the unevenness of the coating could make the sample more susceptible to burning and may also decrease the performance of our samples in flame tests, contributing to some variability of the results. Future work could explore alternative substrates such as metals and investigate the thermal insulation properties of the carbonaceous char layer formed during combustion of the coating.

Although benzoxazine contains many aromatic rings and tertiary amines that contribute minimally to heat release,[44] cardanol-based benzoxazine contains a long, flammable alkyl side chain. Functionalisation of the unsaturated side chain with hydroxyl groups could enhance crosslinking between the phosphate groups in APP and the hydroxyl groups in benzoxazine. This, in turn, may promote the formation of a more stable and protective carbonaceous char layer during combustion.

While changing temperature conditions of the synthesis procedure from 160 °C to 120 °C decreased the viscosity of the resulting product, further characterisation using gel permeation chromatography could be performed. This would provide more insight into the molecular weight distribution of the benzoxazine monomers produced and confirm the minimisation of the early onset of oligomerisation and polymerisation.

5. Conclusions

This work optimises the synthetic route for a cardanol-based benzoxazine and evaluates its potential with APP for fire-retardant coating applications.[9] The benzoxazine was successfully synthesised at 120 °C from cardanol and HMTA within 2 h using standard benchtop equipment. Coatings with varying APP and benzoxazine ratios were prepared and tested. Fire testing showed that increasing the APP content led to a reduced HRR and THR, increased residue formation, and the development of denser char layers. 60% APP and 40% benzoxazine (Sample 6) exhibited the best performance, with a THR of 53 MJ m^{-2}, likely due to improved crosslinking between phosphate and hydroxyl groups and the enhanced flame-retardant effect from the higher APP content.

While these findings demonstrate the potential of cardanol-based benzoxazine with APP in flame-retardant coatings, further investigation is needed to optimise coating properties for practical applications. Due to the thermal sensitivity of wood substrates, alternative substrates should be considered. Additionally, functionalising the alkyl side chains may enable more extensive crosslinking and improve char layer stability during combustion.

6. Materials and methodology

6.1. Materials

All chemicals were used as received. Cardanol (95%) was purchased from Biosynth, USA. Hexamethylenetetramine (HMTA) (>99.0%) was purchased from TCI, Singapore. Ammonium polyphosphate (Exolit AP 435) was purchased from Clariant, Germany. Plywood panels (10 cm × 10 cm × 1.8 cm) and veneered sticks (125 mm × 13 mm × 3 mm) were kindly supplied by Evonik (SEA) Pte Ltd (Evonik Asia Research Hub), Singapore.

6.2. Characterisation of the benzoxazine monomer

To determine the synthesis duration of 2 h, thin layer chromatography was performed on the reaction mixture in 15-minute intervals with an ethyl acetate : hexane volume ratio of 2 : 3 as the solvent.

For structural characterisation of a benzoxazine monomer, NMR spectra were recorded on a Bruker Avance Neo (400 MHz for 1H) using $CDCl_3$ as the solvent. FTIR spectra were obtained using a PerkinElmer Frontier spectrometer, from 4000 cm^{-1} to 400 cm^{-1} with an arithmetic average of 32 scans, where benzoxazine was dripped onto compressed KBr wafers. Viscosity measurements were obtained on an Anton Paar MCR 102e Rheometer with CP 25-2 attachment at a shear rate of 1 s^{-1} to 1000 s^{-1} in 3 min under the ramp linear setting at 25 °C. To evaluate the thermal properties, DSC was performed using a TA Instruments DSC Q10 using aluminium hermetic pans under N_2 flow at a rate of 10 °C min^{-1} from 30 °C to 390 °C. TGA was performed using a Netzsch TG209 F3 and TA Instruments Q500 under N_2 flow in a temperature range of 30 °C to 650 °C.

6.3. Preparation of coating samples

Formulations were mixed according to Table 1, all in mass %. APP and benzoxazine were manually mixed in polypropylene cups before being mixed using a Hauschild DAC 150.1 FVZ K speedmixer at 3000 rpm for 5 min.

For cone calorimeter tests: after the formulations were processed, they were applied onto wood panels (10 cm × 10 cm × 1.8 cm) previously sanded with a #100 sandpaper and dried in a 70 °C oven for a minimum of 2 weeks. A 150-micron wire bar was used to apply the coatings onto the wood substrate. The coated wood panels were then baked in a Binder FD 240 oven at 160 °C for 2 h. A second layer was coated on with the same 150-micron wire bar and the coated wood panels were baked in the oven similarly at 160 °C for 7 h. Three panels were prepared for each formulation.

For UL-94 vertical burning: wood veneered sticks (125 mm × 13 mm × 3 mm) were sanded with a #100 sandpaper and dried in a 70 °C oven for a minimum of 2 weeks. A 150-micron wire bar was then used to apply the coatings onto the substrate. The coated wood sticks were baked in a Binder FD 240 oven at 160 °C for 2 h. After cooling, the sticks were flipped over onto the back side and coated for the second time using a 150-micron wire bar. The sticks were baked again in a Binder FD 240 oven at 160 °C for 2 h. This process was repeated until there were 2 coats per side (front and back). The coated wood sticks were then baked in the oven at 160 °C for 7 h.

For characterisation: the formulated mixtures were dripped onto a stainless-steel substrate and then heated in a Binder FD 240 oven at 160 °C for 7 h. The samples were then scraped off for further analysis.

6.4. Characterisation of coatings

The final dry coating thickness was measured using a Mitutoyo QuantuMike MDH-25 MB micrometer. The average dry coating thickness is available in Table S2 of the SI. Each measurement was taken three times at randomly chosen points on the sample, before coating and after the coating process, respectively. The coating thickness was calculated as ''final thickness of the wood substrate and coating – initial thickness of the wood substrate''. FTIR spectra were obtained using a PerkinElmer Frontier spectrometer from 4000 cm^{-1} to 650 cm^{-1}, using an ATR accessory and the arithmetic average of 32 scans.

To evaluate the thermal properties and flame retardancy of coatings, TGA was performed using a Netzsch TG209 F3 and TA Instruments Q500 under air flow in a temperature range of 30 °C to 650 °C. The cone calorimeter test was performed using a FIREMANA PX07-007, with the set-up in accordance with the ISO 5660 standard, exposed to an external heat flux of 50 kW m^{-2}. The UL-94 vertical burning test was performed following the ISO 1210 standard.

Optical microscopy of burnt samples was performed on an Olympus DSX1000 using 3D acquisition in darkfield mode (3× and 40× lens magnification). Scanning electron microscopy of burnt samples was performed on a FESEM JEOL JSM-7600F in SEI mode with an accelerating voltage of 5.0 kV and a working distance of 8.0 mm.

Conflicts of interest

There are no conflicts to declare.

Data availability

The data supporting this article have been included as part of the supplementary information (SI). Supplementary information is available. See DOI: https://doi.org/10.1039/d5ma01299f.

Acknowledgements

This project was supported by Nanyang Technological University under the URECA Undergraduate Research Programme. L. N. W. T. acknowledges funding from Singapore's MOE Tier 1 (RS14/23).

References

1 R. A. Mensah, L. Jiang, J. S. Renner and Q. Xu, Characterisation of the fire behaviour of wood: From pyrolysis to fire retardant mechanisms, *J. Therm. Anal. Calorim.*, 2023, **148**(4), 1407–1422, DOI: 10.1007/s10973-022-11442-0.
2 J. Song, H. Liang, Y. Cao, M. Wang and Z. Wang, Advancing coatings with polybenzoxazines: insights into molecular design, synthesis, and modification, *J. Mater. Chem. C*, 2024, **12**(25), 9094–9111, DOI: 10.1039/D4TC01351D.
3 N. N. Ghosh, B. Kiskan and Y. Yagci, Polybenzoxazines—New high performance thermosetting resins: Synthesis and properties, *Prog. Polym. Sci.*, 2007, **32**(11), 1344–1391, DOI: 10.1016/j.progpolymsci.2007.07.002.
4 M. Arslan, B. Kiskan and Y. Yagci, Recycling and Self-Healing of Polybenzoxazines with Dynamic Sulfide Linkages, *Sci. Rep.*, 2017, **7**(1), 5207, DOI: 10.1038/s41598-017-05608-2.
5 H. Ishida and H. Y. Low, ''A Study on the Volumetric Expansion of Benzoxazine-Based Phenolic Resin,'', *Macromolecules*, 1997, **30**(4), 1099–1106, DOI: 10.1021/ma960539a.
6 P. S. Gaikwad, *et al.*, Understanding the Origin of the Low Cure Shrinkage of Polybenzoxazine Resin by Computational Simulation, *ACS Appl. Polym. Mater.*, 2021, **3**(12), 6407–6415, DOI: 10.1021/acsapm.1c01164.
7 N. Li, L. Zongyao, Z. Jindong, Y. Jianan, L. Gang and C. Chen, Effect of ammonium polyphosphate and benzoxazine synergistic modification on the flame retardancy of epoxy resin, *Adv. Compos. Mater.*, 1–21, DOI: 10.1080/09243046.2025.2499297.
8 C. H. M. Beraldo, M. R. da Silveira, A. F. Baldissera and C. A. Ferreira, A new benzoxazine-based intumescent coating for passive protection against fire, *Prog. Org. Coat.*, 2019, **137**, 105321, DOI: 10.1016/j.porgcoat.2019.105321.
9 M. M. B. A. Mohamed, Y. X. Ang, R. J. H. Tan, L. S. Tung, X. Xiao, M. Das and L. W. T. Ng, Investigating the fire dynamics of mounted PV weathering effects and material changes, *iScience*, 2025, **28**(10), 113410, DOI: 10.1016/j.isci.2025.113410.
10 H. A. Klfout, A. M. Asiri, K. A. Alamry and M. A. Hussein, Recent advances in bio-based polybenzoxazines as an interesting adhesive coating, *RSC Adv.*, 2023, **13**(29), 19817–19835, DOI: 10.1039/D3RA03514J.
11 H. Ding, X. Wang, L. Song and Y. Hu, Recent Advances in Flame Retardant Bio-Based Benzoxazine Resins, *J. Renewable Mater.*, 2022, **10**(4), 871–895, DOI: 10.32604/jrm.2022.018150.
12 M. L. Salum, D. Iguchi, C. R. Arza, L. Han, H. Ishida and P. Froimowicz, Making Benzoxazines Greener: Design, Synthesis, and Polymerization of a Biobased Benzoxazine Fulfilling Two Principles of Green Chemistry, *ACS Sustainable Chem. Eng.*, 2018, **6**(10), 13096–13106, DOI: 10.1021/acssuschemeng.8b02641.
13 P. Thirukumaran, A. Shakila Parveen and M. Sarojadevi, Synthesis and Copolymerization of Fully Biobased Benzoxazines from Renewable Resources, *ACS Sustainable Chem. Eng.*, 2014, **2**(12), 2790–2801, DOI: 10.1021/sc500548c.
14 E. Calò, *et al.*, Synthesis of a novel cardanol-based benzoxazine monomer and environmentally sustainable production of polymers and bio-composites, *Green Chem.*, 2007, **9**(7), 754–759, DOI: 10.1039/B617180J.
15 M. Monisha, N. Amarnath, S. Mukherjee and B. Lochab, Cardanol Benzoxazines: A Versatile Monomer with Advancing Applications, *Macromol. Chem. Phys.*, 2019, **220**(3), 1800470, DOI: 10.1002/macp.201800470.
16 S. Shukla, A. Mahata, B. Pathak and B. Lochab, Cardanol benzoxazines – interplay of oxazine functionality (mono to tetra) and properties, *RSC Adv.*, 2015, **5**(95), 78071–78080, DOI: 10.1039/C5RA14214H.
17 J. R. Oliveira, D. B. de Freitas, J. F. R. de Oliveira, G. Mele, S. E. Mazzetto and D. Lomonaco, New opportunity for

sustainable benzoxazine synthesis: A straight and convenient one-pot protocol for formaldehyde-free bio-based polymers, *Eur. Polym. J.*, 2021, **156**, 110596, DOI: 10.1016/j.eurpolymj.2021.110596.

18 L. A. Campañone and N. E. Zaritzky, Mathematical analysis of microwave heating process, *J. Food Eng.*, 2005, **69**(3), 359–368, DOI: 10.1016/j.jfoodeng.2004.08.027.

19 S. Farag, A. Sobhy, C. Akyel, J. Doucet and J. Chaouki, Temperature profile prediction within selected materials heated by microwaves at 2.45GHz, *Appl. Therm. Eng.*, 2012, **36**, 360–369, DOI: 10.1016/j.applthermaleng.2011.10.049.

20 G. Cuccurullo, P. G. Berardi, R. Carfagna and V. Pierro, ''IR temperature measurements in microwave heating, *Infrared Phys. Technol.*, 2002, **43**(3), 145–150, DOI: 10.1016/S1350-4495(02)00133-0.

21 J. Green, A Review of Phosphorus-Containing Flame Retardants, *J. Fire Sci.*, 1992, **10**(6), 470–487, DOI: 10.1177/073490419201000602.

22 C. Zhang, *et al.*, Recent trends of phosphorus-containing flame retardants modified polypropylene composites processing, *Heliyon*, 2022, **8**(11), e11225, DOI: 10.1016/j.heliyon.2022.e11225.

23 K.-S. Lim, *et al.*, A review of application of ammonium polyphosphate as intumescent flame retardant in thermoplastic composites, *Composites, Part B*, 2016, **84**, 155–174, DOI: 10.1016/j.compositesb.2015.08.066.

24 Y. Xia, F. Jin, Z. Mao, Y. Guan and A. Zheng, Effects of ammonium polyphosphate to pentaerythritol ratio on composition and properties of carbonaceous foam deriving from intumescent flame-retardant polypropylene, *Polym. Degrad. Stab.*, 2014, **107**, 64–73, DOI: 10.1016/j.polymdegradstab.2014.04.016.

25 Z. Wang, E. Han and W. Ke, Influence of expandable graphite on fire resistance and water resistance of flame-retardant coatings, *Corros. Sci.*, 2007, **49**(5), 2237–2253, DOI: 10.1016/j.corsci.2006.10.024.

26 A. Martos, R. M. Sebastián and J. Marquet, Studies on the ring-opening polymerization of benzoxazines: Understanding the effect of the substituents, *Eur. Polym. J.*, 2018, **108**, 20–27, DOI: 10.1016/j.eurpolymj.2018.08.025.

27 N. Macadam, L. W. T. Ng, G. Hu, H. H. Shi, W. Wang, X. Zhu, O. Ogbeide, S. Liu, Z. Yang, R. C. T. Howe, C. Jones, Y. Y. S. Huang and T. Hasan, 100 m min^{-1} Industrial-Scale Flexographic Printing of Graphene-Incorporated Conductive Ink, *Adv. Eng. Mater.*, 2022, **24**(3), 2101217, DOI: 10.1002/adem.202101217.

28 C. F. Bandeira, A. C. Pereira, E. C. Botelho and M. L. Costa, Benzoxazine resin and their nanostructured composites cure kinetic by DSC, *J. Mater. Res.*, 2013, **28**(22), 3094–3099, DOI: 10.1557/jmr.2013.327.

29 L. Han, *et al.*, Oxazine Ring-Related Vibrational Modes of Benzoxazine Monomers Using Fully Aromatically Substituted, Deuterated, 15N Isotope Exchanged, and Oxazine-Ring-Substituted Compounds and Theoretical Calculations, *J. Phys. Chem. A*, 2017, **121**(33), 6269–6282, DOI: 10.1021/acs.jpca.7b05249.

30 R. Ganfoud, N. Guigo, L. Puchot, P. Verge and N. Sbirrazzuoli, Investigation on the role of the alkyl side chain of cardanol on benzoxazine polymerization and polymer properties, *Eur. Polym. J.*, 2019, **119**, 120–129, DOI: 10.1016/j.eurpolymj.2019.07.026.

31 T. Fateh, T. Rogaume, J. Luche, F. Richard and F. Jabouille, Kinetic and mechanism of the thermal degradation of a plywood by using thermogravimetry and Fourier-transformed infrared spectroscopy analysis in nitrogen and air atmosphere, *Fire Safety J.*, 2013, **58**, 25–37, DOI: 10.1016/j.firesaf.2013.01.019.

32 J. Martinka, P. Rantuch, F. Martinka, I. Wachter and T. Štefko, Improvement of Heat Release Rate Measurement from Woods Based on Their Combustion Products Temperature Rise, *Processes*, 2023, **11**(4), 1206, DOI: 10.3390/pr11041206.

33 Q. Xu, L. Chen, K. A. Harries, F. Zhang, Q. Liu and J. Feng, Combustion and charring properties of five common constructional wood species from cone calorimeter tests, *Constr. Build. Mater.*, 2015, **96**, 416–427, DOI: 10.1016/j.conbuildmat.2015.08.062.

34 K. Li, D. S. W. Pau, J. Wang and J. Ji, ''Modelling pyrolysis of charring materials: determining flame heat flux using bench-scale experiments of medium density fibreboard (MDF), *Chem. Eng. Sci.*, 2015, **123**, 39–48, DOI: 10.1016/j.ces.2014.10.043.

35 R. M. Hadden, Heat Release Rate, in *Encyclopedia of Wildfires and Wildland-Urban Interface (WUI) Fires*, ed. S. L. Manzello, Springer International Publishing, Cham, 2020, pp. 603–610, DOI: 10.1007/978-3-319-52090-2_68.

36 Y. Liu, Q. Ran and Y. Gu, Preparation and properties of benzoxazine blends with intumescent flame retardancy, *Polym. Degrad. Stab.*, 2019, **163**, 15–24, DOI: 10.1016/j.polymdegradstab.2019.02.022.

37 Z.-Q. Qin, Z.-T. Xiao, X.-Y. Lan, X. Wang, Y. Hu and L. Song, Cardanol-derived polybenzoxazine networks integrated with high glass transition temperatures, flame retardancy and toughness, *Polym. Degrad. Stab.*, 2025, **234**, 111232, DOI: 10.1016/j.polymdegradstab.2025.111232.

38 L. W. T. Ng, N. G. An, L. Yang, Y. Zhou, D. W. Chang, J.-E. Kim, L. J. Sutherland, T. Hasan, M. Gao and D. Vak, A printing-inspired digital twin for the self-driving, high-throughput, closed-loop optimization of roll-to-roll printed photovoltaics, *Cell Rep. Phys. Sci.*, 2024, **5**(6), 102038, DOI: 10.1016/j.xcrp.2024.102038.

39 A. K. Y. Low, J. J. W. Cheng, K. Hippalgaonkar and L. W. T. Ng, Self-Driving Laboratories: Translating Materials Science from Laboratory to Factory, *ACS Omega*, 2025, **10**(28), 29902–29908, DOI: 10.1021/acsomega.5c02157.

40 N. G. An, L. W. T. Ng, Y. Liu, S. Song, M. Gao, Y. Zhou, C.-Q. Ma, Z. Wei, J. Y. Kim, U. Bach and D. Vak, Mass-customization of organic photovoltaics and data production for machine learning models precisely predicting device behavior, *Energy Environ. Sci.*, 2025, **18**(21), 9524–9537, DOI: 10.1039/D5EE02815A.

41 S. Doloi, M. Das, Y. Li, Z. H. Cho, X. Xiao, J. V. Hanna, M. Osvaldo and L. W. T. Ng, Democratizing self-driving labs:

advances in low-cost 3D printing for laboratory automation, *Digital Discovery*, 2025, **4**, 1685–1721, DOI: 10.1039/D4DD00411F.

42 L. W. T. Ng, *et al.*, 2D Ink Design, in *Printing of Graphene and Related 2D Materials*, Springer, Cham, 2019, DOI: 10.1007/978-3-319-91572-2_4.

43 A. I. Bartlett, R. M. Hadden and L. A. Bisby, A Review of Factors Affecting the Burning Behaviour of Wood for Application to Tall Timber Construction, *Fire Technol.*, 2019, **55**(1), 1–49, DOI: 10.1007/s10694-018-0787-y.

44 R. Sonnier, *et al.*, Prediction of thermosets flammability using a model based on group contributions, *Polymer*, 2017, **127**, 203–213, DOI: 10.1016/j.polymer.2017.09.012.

45 L. W. T. Ng, *et al.*, Printing technologies, in *Printing of Graphene and Related 2D Materials*, Springer, Cham, 2019, DOI: 10.1007/978-3-319-91572-2_5.